Airborne measurements of electrical atmospheric field produced by convective clouds

P. Laroche

Revue Phys. Appl. **21** (1986) 809-815 DÉCEMBRE **1986**, PAGE 809

Classification
Physics Abstracts
52.80 — 92.90 — 93.85

Airborne measurements of electrical atmospheric field produced by convective clouds (+)

P. Laroche

Office National d'Etudes et de Recherches Aérospatiales, BP 72, 92322 Châtillon Cedex, France

(*Reçu le 28 décembre 1985, accepté le 10 juin 1986*)

Résumé. — Un système de cinq capteurs de champ a été installé sur un avion Transall C160 pour déterminer le champ électrostatique atmosphérique à proximité et à l'intérieur des nuages convectifs. Des mesures ont été effectuées durant la campagne LANDES-FRONT 84 consacrée à l'étude de la convection et des foudroiements. Les calculs effectués à l'aide du système redondant de cinq mesures simultanées, indiquent une assez bonne concordance avec un modèle de champ uniforme, dans le cas de cellules modérément chargées. Des premiers résultats sont présentés et discutés.

Abstract. — A C160 Transall aircraft was equipped with five field mill sensors to provide calculation of the atmospheric electrostatic fields, in the vicinity and inside convective clouds. Measurements were performed during the LANDES-FRONT experiment in 1984. Calculations performed with the redundant five simultaneous measurements indicate a rather good coherence for the uniform field model, in case of moderately electrified cells. Some preliminary results are presented and discussed.

1. Introduction.

A joined ground and in-flight experiment on lightning, and atmospheric electricity associated with convective clouds has been held in the South West of France, in Spring and Summer 1984. The general organization of this experiment is widely described in an other paper (Laroche *et al.*, 1985).

We are specifically concerned here, with the measurements of the electrostatic field in the vicinity and inside the convective clouds. The vertical electrical structure of the convective clouds, which corresponds to a vertical micro physical organization may be analysed by measurements of electrostatic field at ground but, *in situ* measurements are necessary to investigate the actual charge repartition in clouds, and to evaluate maximum field accounted. *In situ* measurements had been performed by instrumented rocket and balloon (Runhke, 1971 ; Winn and Moore, 1971 ; Christian, 1978 ; Chauzy, 1978) but aircraft can be useful for more systematical and more precise spatial analysis. Electrostatic field values must be discussed in relation with the position and the properties of the cloud which are indicated by meteorological radar echoes. For several flights performed with the instrumented C160 Transall aircraft simultaneous ground doppler radars measurements are available. Those data are still processed now.

(+) Cet article a fait l'objet d'une communication à la Conférence Internationale sur la Foudre et l'Electricité Statique (Paris, 10-15 juin 1986).

After a description of the experiment, we present some typical results obtained during the campaign.

2. Description of the experiment.

2.1 INSTRUMENTATION OF THE AIRCRAFT. — The C160 was equipped with microphysical sensors providing the size, shape and concentration of cloud particles (Gayet *et al.*, 1985). Classical temperature measurements were performed. Informations on absolute position of the aircraft and on the three components of the wind are deduced both from inertial plateform data and from on board doppler radar indications.

Local electrical properties of the clouds are indicated by measurements of ion conductivity and electric charge of hydrometers.

The charging of the aircraft due to triboelectric effect is evidenced by two impact sensors installed on the leading edge of the pods supporting the microphysic and electric sensors.

Their front surface is 0.08 m^2 and the range of the associated electronic device is $\pm 50\ \mu A$ corresponding to an average maximum current density of 625 $\mu A/m^2$.

The electrostatic field is measured in five different places of the aircraft fuselage by field-mill type sensors. Field-mill sensor is well adapted to the measurement of the electrostatic field on board aircraft ; it has been widely applied since the end of forties by Gunn (1948), Fitzgerald and Byers (1965), Latham and Stow (1969), Clark (1957), Christian *et al.* (1980), Imianitov (1965), Kasemir (1964) and others. The sensors used for this experiment were firstly set-up on a smaller two engine jet aircraft flown in cirrus cloud to investigate triboelectric effects on aircraft (Boulay and Laroche, 1982). The electrostatic field, penetrating through a grounded grid, is mechanically modulated by a grounded rotating grid (see Fig. 1) ; a plane measuring electrode is exposed underneath to the modulated field and the corresponding ac current is processed by an electronic device providing magnitude and sign of the field. The rotation speed is 12 000 r.p.m. providing a time response of about 10 ms. The heating of the sensor is monitored by a temperature probe, installed inside the sensor head. The field range measurement is typically ± 100 kV/m but, it can be adjusted from ± 10 kV/m to ± 500 kV/m.

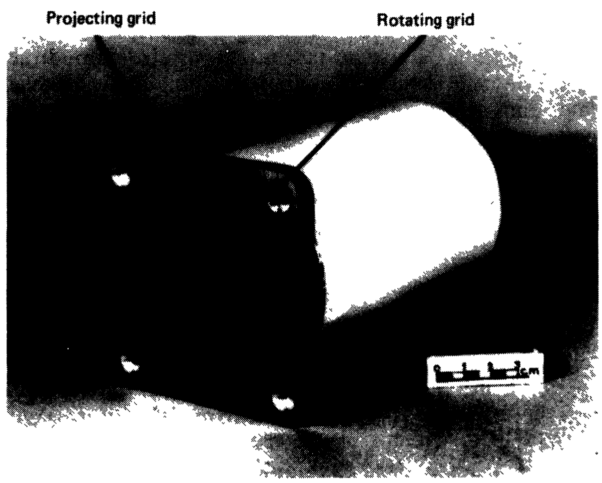

Fig. 1. — Field mill sensor.

2.2 ELECTRIC FIELD AND AIRCRAFT POTENTIAL MEASUREMENTS. — The electrostatic field at the surface of a conducting aircraft is due to the outside atmospheric field and to the net electrical charge on the structure. If it is assumed that there is no interference in the vicinity of the sensor, such as particles impact or corona discharges, the measuring field value E_M is dependent of the three outside field components and the net charge of the aircraft :

$$E_M = \alpha_{Mx} E_x + \alpha_{My} E_y + \alpha_{Mz} E_z + \alpha_{MQ} Q \quad (1)$$

where E_M is the field value delivered by the sensor M ; E_x, E_y, E_z are the field components along three orthogonal axes of the aircraft and Q, is its net charge. The $\alpha_{Mx}, \ldots, \alpha_{MQ}$ coefficients depend on the characteristics of the point M where sensors are set up but they do not depend on charge configuration in clouds if the resulting surrounding field in the vicinity of aircraft may be considered as uniform. In that hypothesis, E_M in equation (1) is a linear function of the outside field components and of the net charge. So, measuring the field in four different places of the aircraft structure, provides a system of four linear equations where the unknown parameters are E_x, E_y, E_z and Q.

This uniform field hypothesis may be rather limitative especially in the case of measurements inside convective clouds. Moreover, for a large aircraft flowing near or inside storm clouds, field enhancement in sharp places provide a low incident field threshold for the corona discharge (few tens of kV/m for a 40 m span aircraft like the C160) ; it seems that redundancy of field measurements are the only way to overcome this problem.

For practical considerations, we limited the experiment on the Transall to five different and simultaneous field measurements. The positions of the sensors on the aircraft were chosen regarding the independence of measurements *versus* incident field, the absence of perturbing equipment and the low structure curvature of the measuring site, and at last (but not at least) the technical difficulties of the setting up (see Fig. 2). The sign of the components of the field is in agreement with the agreement generally applied in atmospheric electricity : a positive charge on one axe of reference (see Fig. 2) induced a positive field in its direction.

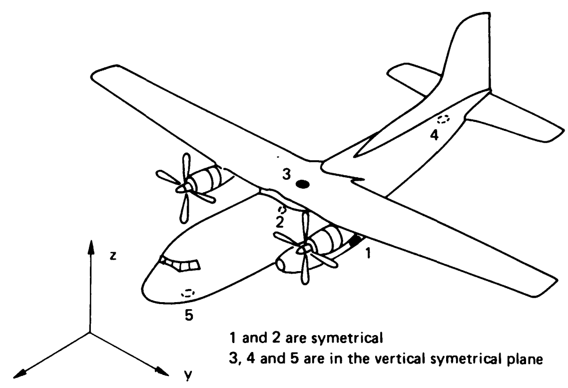

Fig. 2. — Field mill network. 1 and 2 are symmetrical about the fuselage. 3, 4 and 5 are in the vertical plane of symmetry of the aircraft.

The influence coefficients for each measuring point were experimentally determined by electrometric measurements on a 1/100 scale conducting mock up suspended in the 2 m gap of a 4 m by 4 m capacitor : each component of the incidence uniform field is successively applied ; the relative accuracy of the measurements of coefficient is about 2 %.

We can associate to the net charge Q of the aircraft a net potential $V = Q/C$ where C is the capacitance of the aircraft. The value of C measured with the mock up is around 1.2×10^{-9} F.

2.3 DATA PROCESSING. — The analog signals of the five field mills are digitaly sampled at 16 words.s^{-1} and 256 words.s^{-1} rate (12 bit word). The corresponding spatial resolutions are about 6 m and 40 cm, the air speed of the aircraft being about 100 m.s^{-1} during experiment. So those sample rates are sufficient to measure field variations due to electric charges neutralized by atmospheric discharge as well as field variations due to movement of the aircraft.

The atmospheric field and the net potential of aircraft are calculated by direct resolution of one of the five linear system constituted by each set of four measurements. We obtain five determinations of the same parameters, which would have been identical if measurements and model were perfect. The best solution deduced from those five sets of results, in term of the least square fit, is directly derived from the five field measurements :

$$\begin{pmatrix} E_x \\ E_y \\ E_z \\ V \end{pmatrix}_{\text{least square}} = (\tilde{A} \times A)^{-1} \times \tilde{A} \times \begin{pmatrix} E_1 \\ E_2 \\ E_3 \\ E_4 \\ E_5 \end{pmatrix} \quad (2)$$

where A is the 5×4 matrix of the influence coefficients of the five measuring places. The overall quality of the result may be estimated from the dispersion around the least square determination.

We define a quality factor for each component $\left(E_x, E_y, E_z \text{ and } V\right)$:

$$F_x = \frac{1}{5} \sum_{j=1}^{5} \frac{| E_{xLS} - E_{xj} |}{\delta E_{xLS} + \delta E_{xj}} \quad (3)$$

where E_{xLS} is the least square value of the E_x component and E_{xj} the determination of E_x without the j sensor ; δE_{xLS} and δE_{xj} are majorant of measuring errors. If F_x is between 0 and 1, the measurements and the uniform field model are in agreement.

3. Results.

In several cases, electrification is large enough to cause the saturation of one or more of the five field mill sensors ; saturation happens also each time lightning flashes strike the aircraft.

For the experiments in mid developed convective clouds like cumulus congestus, we obtain continuously unsaturated signals.

3.1 SOUNDING OF THE LOWER PART OF A SMALL CELL (Fig. 3). — Electric field and potential variations are observed during about 70 s corresponding to a horizontal displacement of the aircraft of 7 000 m at constant heading. Maximum deviation of the potential is – 1.2 MV during 400 m ; the peak noted A in figure 3 is also noticeable on the vertical electric field component E_z. The three components E_x, E_y and E_z present, respectively, fast small variations corresponding to a typical range of 10 m, large variations on a 400 m scale and global and slow variations due to the overall structure of the cell. The temperature is – 6 °C and the altitude is 2 500 m

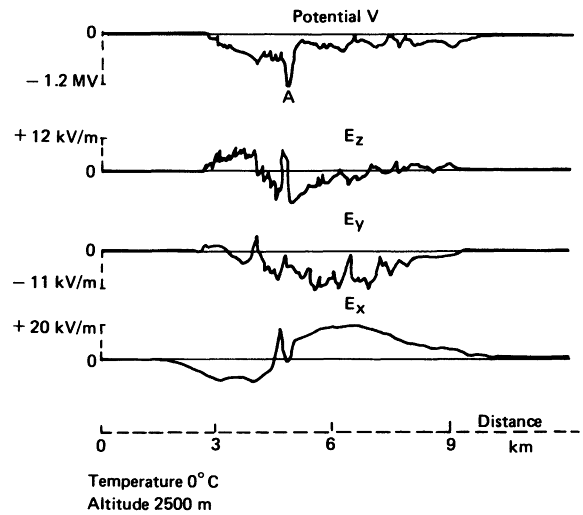

Fig. 3. — Sounding of the lower part of a small cell. Temperature – 6 °C. Altitude 2 500 m.

(750 mb). The outside field has moderate values, between ± 20 kV/m and global variations are unipolar for E_y and bipolar for E_x and E_z.

3.2 SOUNDINGS OF THE UPPER PART OF A SMALL CELL (Fig. 4). — Two successive soundings are carried out at constant level (temperature – 21 °C, altitude 4 900 m, static pressure 550 mb), in the upper part of a cell, the top of which being visually estimated around 5 500 m.

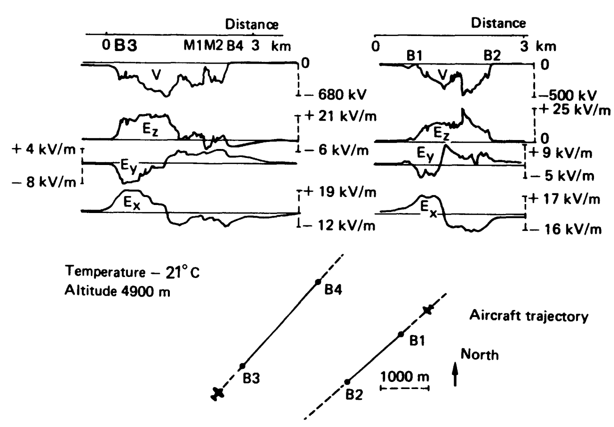

Fig. 4. — Two soundings near the top of a small cell.

For the first sounding, the duration of signals is around 15 s indicating a thickness of 1 500 m. The potential remains negative with a moderate maximum magnitude of – 580 kV. About in the middle of the sequence, a natural lightning flash occurs inducing a fast variation of the aircraft potential and of the vertical component of the field ; no corresponding effect is noticeable on the E_x and E_y components. This flash neutralized a charge beneath or above the aircraft. E_z is positive and unipolar (maximum value 25 kV/m) ; E_x and E_y are bipolar (maximum value 17 and 8 kV/m). E_x variation is smooth ; oscillations are superimposed on the E_z and E_y variations with a corresponding spatial range from 10 to 200 m.

The field and potential variations obtained with the second sounding are of the same nature. Maximum potential magnitude is 680 kV. E_z is positive during the first part of the sounding (max. 21 kV/m) and oscillates to -6 kV/m, 500 m before the end of the sounding. E_x and E_y are bipolar ; their magnitudes are close to those measured during the first sounding.

4. Discussion.

Limitations and perturbations of electrostatic field measurements are due to the size of the measuring vector (the aircraft), to the triboelectric effect and to the emission of corona discharges.

By amplifying the atmospheric field in an area surrounding it, the aircraft may modify the behaviour of charged cloud particles closed to it.

For high field, corona breakdowns of both signs occur from the sharpest parts of the aircraft. Gazeous ions emitted, attach to small cloud particles like droplets. The resulting low mobile space charge is mixed in the vortexes of the air flow behind the aircraft. As the aircraft potential has limited values, this space charge is neutral and we may infer that its contribution to the field is weak. But, the electrical shape of the aircraft may be drastically modified by those discharges governed by the airflow and the electric field. To attenuate this perturbating effect one can either use a high corona threshold measuring vector like an ideal sphere (Few, 1978), either, as we try to do on the C160, place the measuring sites as far as possible from places like wings tips or propellers, where corona discharges are supposed to occur first.

Triboelectric effect may cause a similar problem, complicated by the fact that charged hydrometers displaced by air flow, may evoluate near the measuring sites whatever their protections against corona are.

Independently of the effect of the aircraft on the cloud medium, the use of the uniform field model limits the size of the phenomenon that can be analysed by a 40 m span aircraft like the C160 : if, for instance, the aircraft penetrates a vertical charged zone of few tens of meters, its active structure can not be accurately calculated.

Behaviour of the uniform field model. — As exposed in section 3, the validity of the uniform field interpretation of the measurements can only be discussed by use of a redundant set of field values. The five measurements on the aircraft provide five distinct determinations the quality of which, in the calculation of the four unknown parameters, is different. This quality depends on the position, on the aircraft, of the four measuring sites used for the calculation.

Three, among the five sensors, are set up in the vertical plane of symmetry, and therefore, are not influenced by the horizontal component E_y of the field, orthogonal to the trajectory of the aircraft ; obviously, E_y calculation excluding one of the two influenced sensors, would be less significative. If, for a given configuration, the parameter P_i (one of the field components or the potential) is calculated by the following expression :

$$P_i = \sum_{j=1}^{4} \alpha i j n_j \tag{4}$$

(n_j are the four considered measurements), we can majorate the error on P_i by :

$$\Delta P_i = \sum_{j=1}^{4} | \alpha i j | \Delta n_j \tag{5}$$

where Δn_j is the absolute error on measurement n_j, including sensor and site calibration errors. Assuming an identical absolute error for the measurement, we can predict the quality of the calculation by the value :

$$\Delta P_{im} = \sum_{j=1}^{4} | \alpha i j | . \tag{6}$$

Table in figure 5 gives the ΔP values for all the configurations and for each component. The greater the ΔP values the less significative the corresponding calculation is.

So, as qualitatively inferred above, configurations 1 and 2, excluding one of the sensor directly influenced by E_y, have ΔP values, for this component, twice those of other configurations. Similarly, configuration 3 seems very bad for calculation of E_z and V ; configurations 1 and 2, with this criteria, seem to be the best for E_x calculation. For all the components, ΔP values corresponding to the least square calculation, are very close to the lowest one.

	ΔP				
	configuration # 1 2	3	4	5	Least square
E_x	.37 kV/m	.63 kV/m	.68 kV/m	.72 kV/m	.39 kV/m
E_y	1.53 kV/m	.7 kV/m			.7 kV/m
E_z	.71 kV/m	5.26 kV/m	.68 kV/m	.75 kV/m	.68 kV/m
V	16.9 kV	127 kV	21.2 kV	17.8 kV	17 kV

Fig. 5. — Behaviour of the field and potential calculations. Configuration no i is made with all but minus the i measurements. ΔP correspond to maximum errors of calculation for an absolute measuring error of 1 kV/m for each measurement.

True behaviour of the measurement is illustrated by the table in figure 6 on which is indicated the mean value per second of the calculations, during six seconds corresponding to portion $M_1 M_2$ of the trajectory of the aircraft (see Fig. 4).

CONFIGURATION # 1	2	3	4	5	least square	F	point #
E_x (kV/m)							
- 9.1		- 11.6	- 11.9	- 6.8	- 9.3	1.87	1
- 5.1		- 5.9	- 6	- 4.4	- 5.2	.72	2
- 3.8		- 3.9	- 3.9	- 3.7	- 3.8	.065	3
- 2.8		- 2.6	- 2.6	- 3	- 2.8	.15	4
- 5.7		- 6.6	- 6.7	- 4.8	- 5.8	.85	5
- 4.7		- 5.7	- 5.9	- 3.8	- 4.8	1.3	6
E_y (kV/m)							
- 2.3	8.9	3.3			3.3	1.7	1
.9	4.2	2.5			2.5	.56	2
2.5	2.8	2.6			2.6	.055	3
3.1	2.1	2.6			2.6	.13	4
1.2	3.5	3.2			3.2	.65	5
1.2	5.6	3.4			3.4	.95	6
E_z (kV/m)							
4.7		- 17.1	3.2	2.5	3.1	1.86	1
4,9		- 1.7	4.4	4.2	4.4	.6	2
6.4		5.6	6.3	6.3	6.3	.057	3
4.6		6.5	4.8	4.8	4.8	.14	4
.5		- 7.5	0	- .3	0	.8	5
- 2.6		- 11.3	- 3.2	- 3.5	- 3.2	1.51	6
V kV							
270		- 210	331	308	280	1.83	1
351		207	370	363	354	.6	2
448		431	450	450	448	.056	3
413		454	408	410	412	.14	4
263		85	286	277	267	.78	5
119		- 73	144	135	123	1.4	6

Fig. 6. — Field and potential values between points M_1 and M_2 of figure 4.

For each set of calculation, the corresponding factor of quality determined by expression (3) is indicated. It can be seen that configuration 3 for E_z and V is far from the others, confirming the above remarks. No evident conclusion can be proposed for E_y calculation because, in fact, we have only three different determinations. E_x calculations for the three best configurations according ΔP values are almost identical.

More generally, these data suggest two remarks. Firstly, when the quality factor F is lower than unity, indicating a good fit to the uniform field model, actual dispersions on all calculations are weak : even the *bad configurations* fit.

Practically, it appears that fitting between *good configurations* remains correct even for values of F which are closed to two.

Secondly, the differences between each configuration have a constant sign (apart in the case of the very bad configuration 3 for E_z and V). This fact, which is a general result, suggests that a slight and systematical inadequacy of the uniform model occurs that may be due to differences between the mock up used for calibration and the actual shape of the aircraft.

Atmospheric field and aircraft potential values. — Due to saturation of the sensors, the range of the field and potential measurement for this campaign was :

$$V_{\max} = \pm 1.9\ \text{MV},\ E_{x\max} = \pm 55\ \text{kV/m},$$

$$E_{y\max} = 70\ \text{kV}/\text{m and } E_{z\max} = \pm 73\ \text{kV/m}.$$

During flights in high electrified clouds, these saturation values are obtained frequently. Except during close or direct lightning, potential remained negative indicating that the aircraft is negatively charged. Evolutions of potential are due both to field-induced corona charging and triboelectric charging.

The curves in figure 7 (a) correspond to a low level impact current : no correlation between current and aircraft potential appears in that case neither in magnitude nor in sign. Figure 7 (b) is a typical case of an intense triboelectric regime, for which there is evidence of a strong correlation between current and potential.

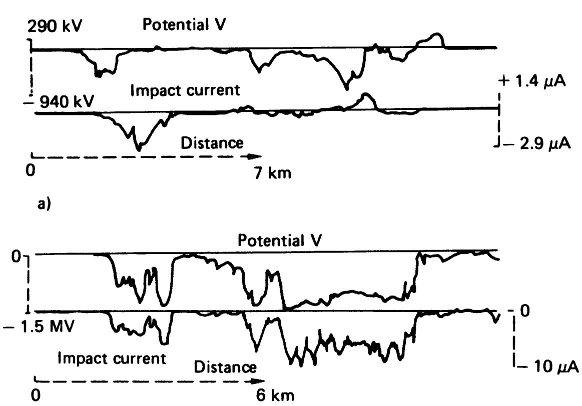

Fig. 7. — Impact current. (a) Low activity. (b) High activity.

Field values must be discussed together with microphysical informations and global radar characterization of the cells and that will be possible, for data collected during this campaign. The two typical examples in figures 3 and 4 indicate a general agreement of the field values with the global characteristic of the vertical charge separation in a convective cloud. For a sounding near the base of a cell (Fig. 3), we obtained a bipolar variation of the vertical field (± 12 kV/m), the first part of the sounding indicating a positive field which may correspond to the low altitude positive charge often detected around the 0 °C level. Negative value for E_z corresponds to negative charge in excess above the aircraft. The E_y global unipolar variation and the corresponding E_x bipolar variation are somewhat consistant with a monopole charge model (about -4 C at 2 km left of the trajectory).

The two soundings in figure 4 are carried out at five minutes interval, near the top of a same cell around the -21 °C level. Values and sign of the field components correspond to a globally positive medium above and at the level of the trajectory. For the second part of the B_3 B_4 sounding, E_z is negative indicating that positive charge is centred below the trajectory.

Both in figures 3 and 4, we observe field variations corresponding to charged area of small dimension (200-400 m).

The charge distribution corresponding to the electric field is not, in general, clearly evidenced by individual horizontal sounding. A complete mapping of the field is, in theory, necessary to calculate the electrical charge density, according to Poisson's law :

$$\operatorname{div} \mathbf{E} = \frac{\rho}{\varepsilon_0} \tag{7}$$

where $\mathbf{E}$ is the electric field, ρ is the volumic density of charge and ε_0 the permittivity of vacuum. Nevertheless, we observed certain soundings for which direct interpretation is possible, by fitting a simple electrostatic model with the measurements. That is the case for the results presented in figure 4. Figure 8 shows mean values of the horizontal and vertical components of the field, calculated each second, and superimposed on the trajectory of the aircraft, for the portion B_1 B_2 of the flight. As mentioned above, the vertical component may be due to a net positive charge above the aircraft. The horizontal field, beyond the point B_1 is constant along about 500 m of the trajectory : it points in constant direction ; the horizontal field then reverses within 200 m and stay rather constant along the next 600 m, indicating the same value that before the inversion by pointing in the opposite direction. This field pattern may be due to a vertical charge distribution of 200 m thickness, perpendicular to the field direction and indicated by the two dash lines in figure 8. According to equation (1), we have in that case :

$$\rho = 2\,\varepsilon_0 \frac{E}{h} \tag{8}$$

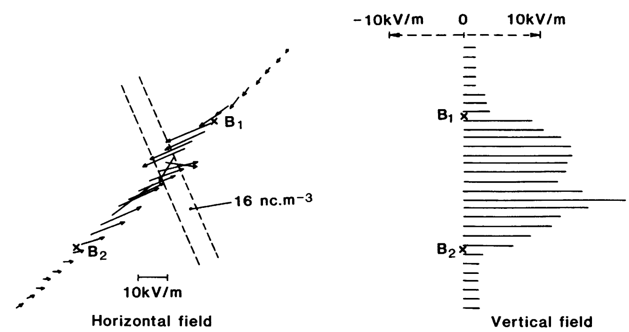

Fig. 8. — Electric field along B_1 B_2 path.

where E is the value of the constant field and h the thickness of the charge layer. The corresponding mean value for ρ is 16 nC. m^{-3} which is a rather high charge density but is quite compatible with charges that may be worn by drop : for instance, ρ may be due to drop wearing 4 pC for a concentration of 4×10^3 m^{-3}.

5. Conclusions.

Atmospheric field and aircraft potential have been measured with a five field mill network installed on the fuselage of a Transall C160 aircraft. Calculations use a uniform field model. The redundancy of measurements have been used to verify the validity of the model : it fits with measurements for medium intensity fields (few tens of kV/m) ; the characteristics of the network installed on the Transall are that potential, longitudinal and vertical field are well determined but the transversal field calculation is less precise.

Space charge distribution may be deduced from field calculation for soundings providing a clear correspondence with simple electrostatic models. For those cases, we shall carry on our study by comparing electric measurements and microphysical sensors on the aircraft and by radar informations obtained from the ground.

6. Acknowledgments.

This work is supported by DRET (Direction des Recherches et Etudes Techniques. French DOD).

References

[1] BOULAY, J. L., LAROCHE, P., *Aircraft potential variations in flight,* International Aerospace and Ground Conference on Lightning and Static Electricity (Oxford) 1982.

[2] CHAUZY, S., Une méthode de mesure de la composante horizontale du champ électrique à l'intérieur des nuages, *J. Rech. Atmos.* **9** (1975) 127.

[3] CLARK, J. F., Airborne measurement of atmospheric potential gradient, *J. Geophys. Res.* **62** (1957) 64.

[4] CHRISTIAN, H. J., *Vector electric field structure inside a New Mexico thundercloud,* Ph. D. Th., Rice University (Houston, Texas), 1978.

[5] CHRISTIAN, H. J., HOLMES, C. R., BULLOCK, J. W., GASKELL, W., ILLINGWORTH, A. J., LATHAM, J., Airborne and ground-bases studies of thunderstorms in the vicinity of Langmuir Laboratory, *Quart. J. Met. Soc.* **106** (1980).

[6] FEW, A. A., WEBER, M. E., CHRISTIAN, H. J., *Vector electric field measurement in thunderstorms,* Conference on Cloud Physics (Issaquah Washington) 1978.

[7] FITZGERALD, D. R., BYERS, H. R., *Aircraft electrostatic measurement instrumentation and observations of cloud electrification,* Coroniti Editor (Elsevier Publishing Company) 1965.

[8] GAYET, J. F., DUROURE, C., SOULAGE, G., LAROCHE, P., *Location of lightning strokes on aircraft in storm field with measured electrical, microphysical and dynamical properties,* International Aerospace and Ground Conference on Lightning and Static Electricity (Paris) 1985.

[9] GUNN, R., Electric field intensity inside of natural clouds, *J. Am. Phys.* **9** (1948).

[10] IMIANITOV, I. M., The electrical structure of thick convective clouds and its relation to motion of air in clouds, *J. Am. Met. Soc.* (1965) 241.

[11] KASEMIR, H. W., The cylindrical field mill, Tech. Rep. ECOM 2526 (1964).

[12] LATHAM, J., STOW, C. D., Airborne studies of the electrical properties of large convective clouds, *Quart. J. R. Met. Soc.* **95** (1969).

[13] LAROCHE, P., DILL, M., GAYET J. F., FRIEDLANDER, M., *In flight thunderstorm environmental measurements during the Landes 84 campaign,* International Aerospace and Ground Conference on Lightning and Static Electricity (Paris) 1985.

[14] RUNHKE, L. H., A rocket borne instrument to measure electric fields inside electrified clouds, NOAA Tech. Rep. TR-ERL 206 APCL-20 (1971).

[15] WINN, W. P., MOORE, C. B., Electric field measurements in thunderclouds using instrumented rockets, *J. Geophys. Res.* **765** (1971) 21.